PCCP

ROYAL SOCIETY OF CHEMISTRY

PAPER

View Article Online
View Journal | View Issue

Cite this: *Phys. Chem. Chem. Phys.*, 2025, **27**, 7556

Isomerisation of phosphabutyne and a photochemical route to phosphabutadiyne (HC_3P), a phosphorus analogue of cyanoacetylene†

Arun-Libertsen Lawzer, *[a] Elavenil Ganesan, [a] Thomas Custer, [a] Jean-Claude Guillemin [b] and Robert Kołos [a]

Received 31st October 2024,
Accepted 24th January 2025

DOI: 10.1039/d4cp04182h

rsc.li/pccp

The photochemistry of phosphabut-1-yne, CH_3CH_2CP, was investigated by means of infrared spectroscopy assisted by theoretical (DFT) predictions. The UV-irradiated compound, isolated in a cryogenic argon matrix, undergoes isomerization and dissociation. Several isomers of phosphabutyne, in addition to phosphabutadiyne (HC_3P), ethynylphosphinidene (HCCP), and phoshaethyne (HCP) are formed as the main photoproducts. Vibrational spectra of astrochemically relevant molecules HC_3P and CH_2CHCP (vinylphosphaethyne), have been detected and analyzed here for the first time.

Introduction

Phosphaalkynes and phosphaalkenes are reactive molecules which have been used as synthetic building blocks for more than a decade.[1–4] Following the generation of phosphaethyne (H–C≡P, the phosphorus analogue of hydrogen cyanide) by Gier,[5] several other kinetically unstable phosphaalkynes (*e.g.* N≡C–C≡P, HC≡C–C≡P and H_2C=CH–C≡P) were produced using flow pyrolysis and detected using microwave spectroscopy.[6–9] Without appropriate, bulky stabilizing substituents, most of these molecules with phosphorus–carbon multiple bonds undergo oligomerization,[10–13] making the smallest of them difficult to synthesize under normal laboratory conditions. *tert*-Butyl-substituted phosphaethyne (3,3′-dimethylphosphabutyne) was the first molecule with a phosphaalkyne unit synthesized.[14,15] Given that cyanoacetylene[16] and vinyl cyanide[17] are commonly detected interstellar molecules, the spectroscopy of their P-bearing analogues phosphabutadiyne (HC_3P) and vinylphosphaethyne (CH_2CHCP) is also of interest to astrochemistry. To date, only a few phosphorus containing molecules have been detected in the interstellar medium: CP radical,[18] HCP, PN, PO radical, CCP radical, and tentatively, NCCP.[19,20] Phosphaalkenes and phosphaallenes, just like phosphaalkynes, are kinetically unstable unless stabilized with bulky, electron-rich substituents.[21–25] Phosphaethene (CH_2=PH) has been characterized with microwave spectroscopy[26,27] and two of its IR bands were tentatively identified.[28] The simplest phosphaallene CH_2=C=PH was proposed as an intermediate in base-catalyzed thermal rearrangements of alkynylphosphines to phosphaalkynes[29] (Scheme 1(a)) and later characterized as a photoproduct of phosphapropyne rearrangement in an argon matrix.[30]

The cryogenic technique of rare-gas matrix isolation provides the opportunity to characterize reactive molecules often classified as intermediates.[31] In solid argon, UV-photolyzed phosphapropyne undergoes rearrangement and dehydrogenation to form molecules such as phosphaallene and triplet ethynylphosphinidene (HCCP)[30] (Scheme 1(b)). Phosphinidenes are phosphorus analogues of nitrenes and our knowledge of these intermediate species is growing slowly but still limited to just a few compounds.[32] In this context, it was of interest to explore the photochemistry of phosphabut-1-yne, CH_3–CH_2–C≡P (hereafter phosphabutyne or **1**) as a way to obtain HC_3P, CH_2CHCP, open-shell organophosphorus species,

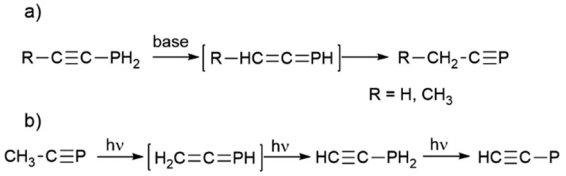

Scheme 1 Rearrangement of alkynylphosphines (a)[29] and phosphapropyne (b).[30]

[a] *Institute of Physical Chemistry, Polish Academy of Sciences, Ul. Marcina Kasprzaka 44/52, 01-224, Warsaw, Poland. E-mail: alawzer@ichf.edu.pl, eganesan@ichf.edu.pl, tcuster@ichf.edu.pl, rkolos@ichf.edu.pl*
[b] *University of Rennes, Ecole Nationale Superieure de Chimie de Rennes, CNRS-IRCR, 6226, F-35000, Rennes, France. E-mail: jean-claude.guillemin@ensc-rennes.fr*

† Electronic supplementary information (ESI) available. See DOI: https://doi.org/10.1039/d4cp04182h

and other phosphorus-containing unsaturated molecules of potential interest for spectroscopy of reactive intermediates and astrochemistry. Particularly important was the goal to investigate the completely unexplored infrared spectroscopy of HC_3P and CH_2CHCP. Thus far, only the microwave, *i.e.* purely rotational transitions of these two molecules have been reported.

The characterisation of the molecular vibrations of such exotic phosphorus-bearing molecules is of interest to the rapidly growing field of IR astrospectroscopy.[33]

Results and discussion

Photochemistry and isomerization of phosphabutyne

Irradiation of phosphabutyne (**1**) at 254 nm induces isomerization (hydrogen and/or methyl group migration) and dissociation. We characterized the species indicated in Scheme 2. Product ratios could be varied by using additional precursors and radiation sources, allowing us to distinguish products and their corresponding IR spectra. Most of the IR bands of the species (Scheme 2) formed through the UV-photolysis of **1** have been identified (ESI,† S10). The presence of 1-propynylphosphine **3**, propadienylphosphine **5**, and propargylphosphine **6** was confirmed with IR absorption spectra of the authentic substances (obtained through preparative synthesis) isolated in argon matrices. Spectra measured during the photolysis of **1**, combined with theoretical (DFT) predictions of band frequencies and intensities, made it possible to follow the time evolution of the relative concentrations of photoproducts (Fig. 1).

Subsections below describe the details pertaining to identification of the individual molecules. DFT-predicted IR spectral parameters for species **1**, **2a**, **2b**, **4**, and **6**, as well as the listing of bands observed for Ar matrix-isolated authentic compounds **3**, **5**, and **6** are provided as ESI.†

Phosphaallenes $CH_2{=}C{=}P{-}CH_3$ (2a) and $CH_3{-}CH{=}C{=}PH$ (2b)

Substituted phosphaallenes such as 1-methyl-1-phosphaallene, **2a** and 3-methyl-1-phosphaallene, **2b** are the products of methyl group and hydrogen atom migration in **1**, respectively. Their appearance among the photoproduced isomers is analogous to that of phosphaallene ($CH_2{=}C{=}PH$) in the course of phosphapropyne (CH_3CP) photolysis.[30]

The P–H bending, P–H stretching, and C=C stretching modes of **2b** appear at 884.3 cm^{-1}, 2257.6 cm^{-1} and 1753.5 (broad) cm^{-1}, respectively, close to the values reported for the unsubstituted phosphaallene[30] (888.4 cm^{-1}, 2264.4 cm^{-1} and 1732.9 cm^{-1}). The bands due to the allenic C–H in-plane and out-of-plane bendings of **2b** appear at 1262.1 cm^{-1} and 808.7 cm^{-1}, respectively. Methyl unit bending bands around 1400 cm^{-1} are the weakest and difficult to assign due to the overlapping features of other products. Synthesis of the species **2a** has been reported and some of its IR bands were measured at 77 K.[34] The C=C stretching bands of these phosphaallenes conveniently fall within an uncongested region allowing for reliable identification. The band reported for solid **2a** at 77 K[34] had a maximum at 1715 cm^{-1}, while in the argon matrix we detect two peaks: 1715.8 cm^{-1} and 1737.4 cm^{-1}, which probably reflect separate microenvironments (matrix "sites"). The CH_2 wagging mode of the allenic unit in solid **2a** was reported at 869 cm^{-1}; in argon matrix it appears at 858.2 cm^{-1}. Optical densities of the IR absorption features assigned to **2a** are mutually correlated, as are those assigned to **2b** and the corresponding frequencies agree well with the DFT predictions (Fig. 2 and ESI,† S2.3, S3.3). The time evolution curves (Fig. 1) indicate that both species are formed in the early stages of the photolysis. The *P*-methylated molecule **2a** seems to be more photostable than **2b**. Within our proposed reaction pathway (Scheme 2), **2b** is a key intermediate species for consecutive photochemical transformations.

Propynylphosphine $CH_3{-}C{\equiv}C{-}PH_2$ (3)

According to DFT predictions, propynylphosphine (**3**) is the most thermodynamically stable structural modification among the isomers of phosphabutyne, and it is reasonable to expect a photoinduced transformation from **1** to **3**, analogous to the

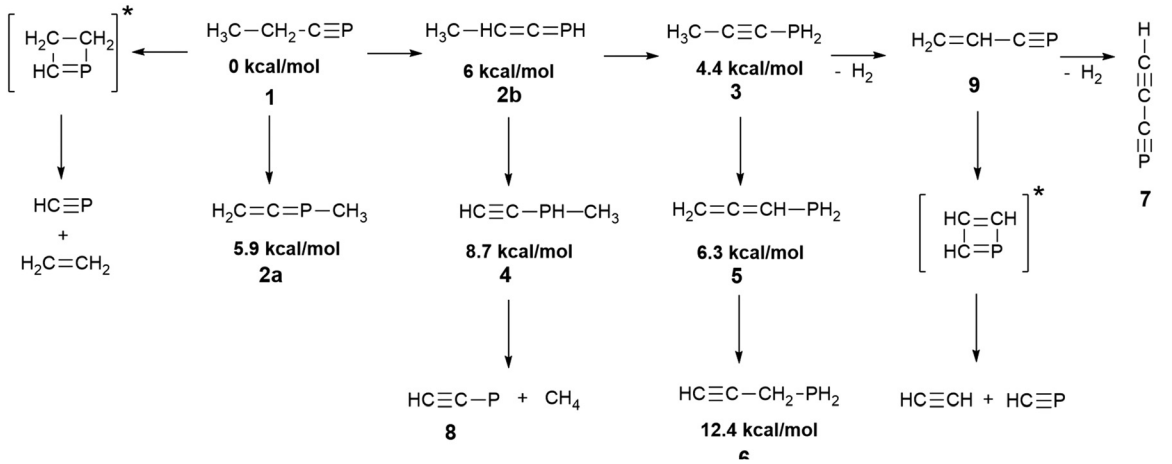

Scheme 2 Products formed in the 254 nm photolysis of phosphabutyne in solid argon. The placement of the arrows, while compatible with Fig. 1 and 7, is provisional. DFT-derived relative electronic energies of the isomers of C_3H_5P species are provided.

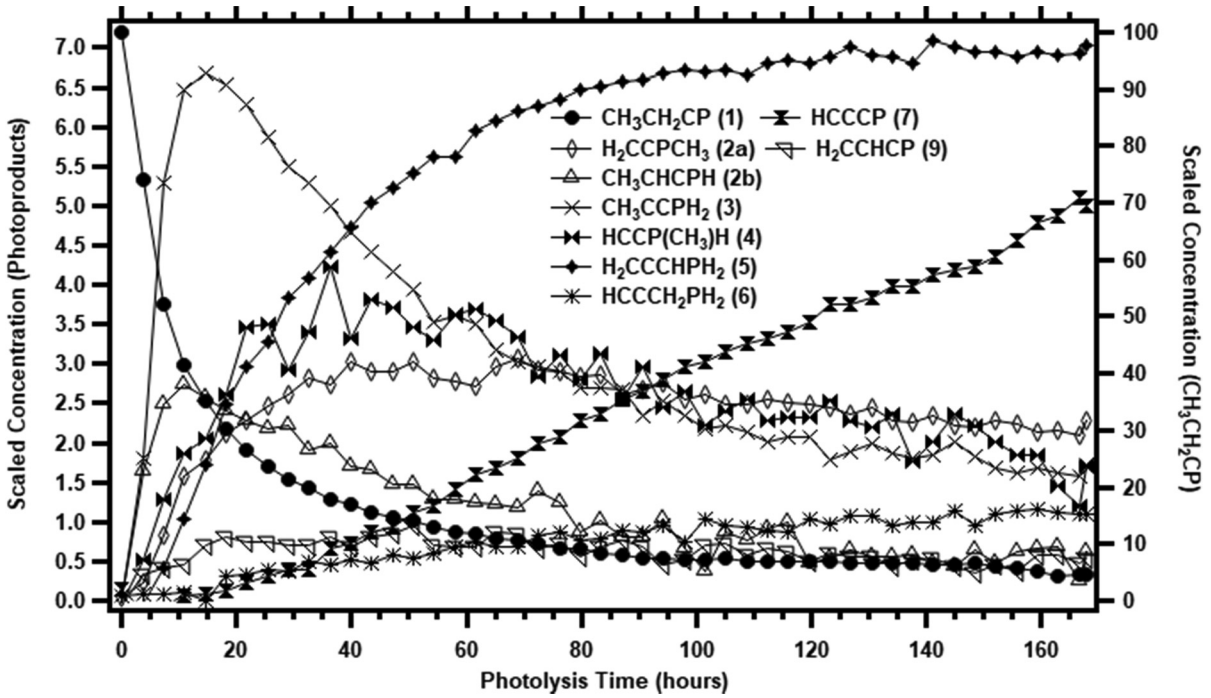

Fig. 1 Isomerization (**1–6**) and dehydrogenation (**7**,**9**) products traced over the course of 254 nm photolysis of phosphabutyne (**1**) in solid Ar, scaled with respect to the initial concentration of the precursor, taken as 100. Integrated intensities measured for the bands centered at 1551.2 cm^{-1} (**1**), 858 cm^{-1} (**2a**), 809 cm^{-1} (**2b**), 2216.9 cm^{-1} (**3**), 629 cm^{-1} (**4**), 831 cm^{-1} (**5**), 635 cm^{-1} (**6**), 1524.3 cm^{-1} (**7**), and 924 cm^{-1} (**9**) were used in conjunction with the B3LYP/aug-cc-pVTZ-derived absolute IR band strengths of 38.7 km mol^{-1} (**1**), 44.1 km mol^{-1} (**2a**), 20.2 km mol^{-1} (**2b**), 34.2 km mol^{-1} (**3**), 40.7 km mol^{-1} (**4**), 52.6 km mol^{-1} (**5**), 20.0 km mol^{-1} (**6**), 35.7 km mol^{-1} (**7**), and 44.8 km mol^{-1} (**9**).

rearrangement of CH_3–C≡P to HC≡C–PH_2.[30] Here, **3** appeared as the main product at the early stages of the photolysis, but decayed almost completely upon prolonged irradiation (Fig. 1 and 3). Its identification was straightforward, given the perfect match with the spectrum of pure **3** in solid argon (Fig. 3). The species is likely formed *via* a two-step 1,3-hydrogen migration, passing through **2b**. Hg-lamp photolysis of the matrix isolated authentic sample of **3** produces a mixture of photoproducts very similar to that obtained from **1** (ESI,† S4.4).

Ethynylmethylphosphine HC≡C–PH–CH_3 (4)

Species **4** is presumably formed from **2a** through 1,3-hydrogen migration and/or from **2b** through 1,3-methyl group migration towards the phosphorus center. IR bands of this molecule appear mostly as multiplets and are located in congested

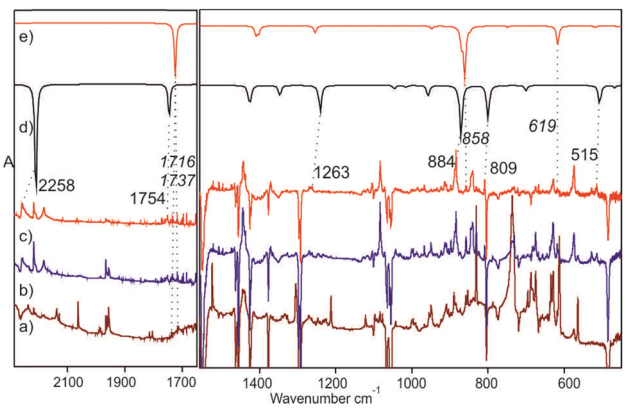

Fig. 2 Identification of 1-methyl-1-phosphaallene **2a** and 3-methyl-1-phosphaallene **2b** among the phosphabutyne **1** photolysis products in solid argon. Traces (a)–(c) are difference spectra (after-minus-before photolysis) showing the net effects of, respectively, 76 h, 3 h and 1.5 h of Hg-lamp irradiation; traces (d) and (e) are B3LYP/aug-cc-pVTZ predictions (frequency scaled by 0.96) for **2b** and **2a**, respectively. Numbers give the band wavenumbers assigned to **2a** (italicized) and **2b**.

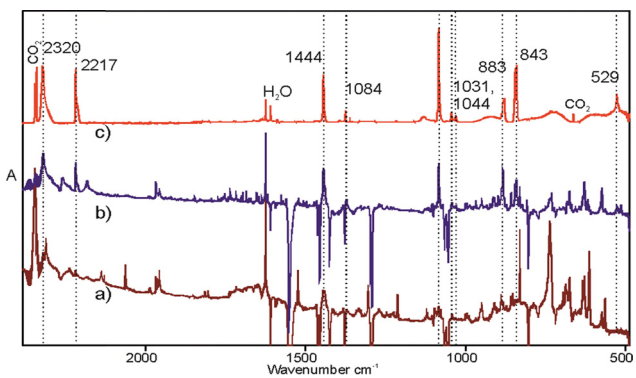

Fig. 3 Identification of propynylphosphine **3** among the phosphabutyne **1** photolysis products in solid argon. Traces (a) and (b) are difference spectra (after-minus-before photolysis) showing the net effects of, respectively, 76 h and 3 h of Hg-lamp irradiation (concentration of **3** peaks at the beginning photolysis); trace (c) represents the spectrum of pure **3** isolated in solid Ar. Numbers give the band wavenumbers assigned to **3**.

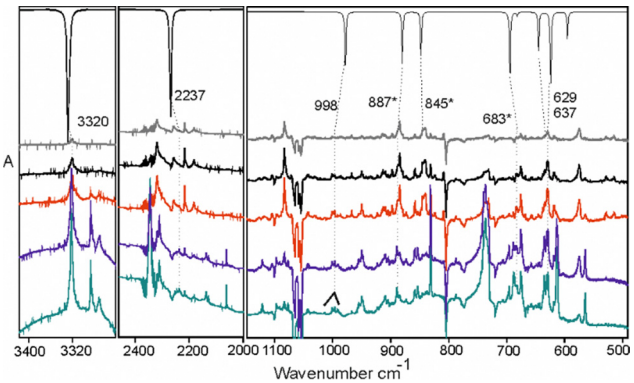

Fig. 4 Identification of ethynylmethylphosphine (**4**) among the phosphabutyne (**1**) photolysis products in solid argon. Topmost trace shows the B3LYP/aug-cc-pVTZ prediction for the IR spectrum of **4** (frequency scaled by 0.96). The other five traces are difference spectra (after-minus-before photolysis) illustrating (bottom to top) the net effect of 76 h, 46 h, 12 h, 6 h and 1.5 h of Hg-lamp irradiation. Numbers give the band wavenumbers assigned to **4** (spectral congestion makes the asterisked assignments less certain).

spectral regions. The C–H stretching vibration of the acetylenic unit of **4** overlaps the C–H stretchings of **6** and **7** (ESI,† S5.3b). A good candidate for the respective C–H bending band emerges prominently at 629.1 cm^{-1}, in good agreement with the DFT prediction (Fig. 4 and S5.3a, ESI†). The PH stretching of **4** reported[34] at 2260 cm^{-1} may correspond to a weak band observed at 2237.2 cm^{-1}. The C–H stretching band at 3320.2 cm^{-1}, a candidate for the main IR feature of **4**, is observable at initial stages of the photolysis. Later on, however, it becomes overlapped by the much stronger C–H stretching band of HC_3P (**7**) at 3322.7 cm^{-1} (ESI,† S5.3b). Considering the uncertainties, our identification of **4** (Fig. 4) is only tentative.

Propadienylphosphine $CH_2{=}C{=}CH{-}PH_2$ (5)

Species (**5**) appears as one of two major products of the photolysis (along with HC_3P). Accordingly, of all the observed

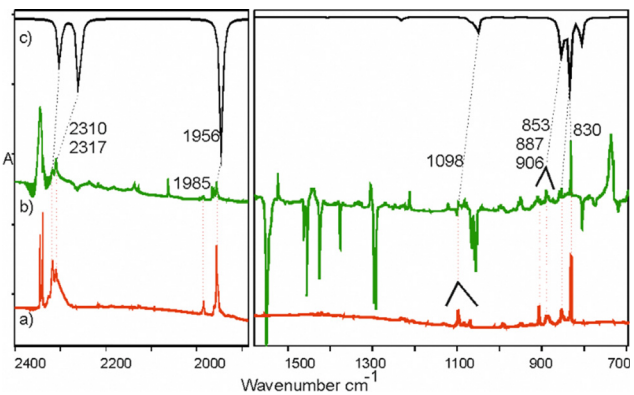

Fig. 5 Identification of propadienylphosphine (**5**) among the phosphabutyne (**1**) photolysis products in solid argon. Trace (a) represents the spectrum of an authentic (synthesized) sample of **5** isolated in solid Ar. Trace (b) is the difference spectrum (after-minus-before photolysis) showing the net effects of 76 h of Hg-lamp irradiation; traces (c) illustrate B3LYP/aug-cc-pVTZ predictions (frequency scaled by 0.96) for **3**. Numbers give the band wavenumbers assigned to **5**.

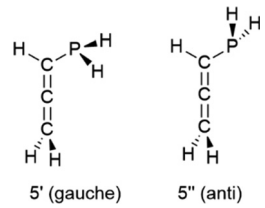

Scheme 3 Rotamers of **5**.

C_3H_5P isomers, this species appears to be the least susceptible to any decomposition induced by 254 nm radiation. Species **5** may be formed *via* a 1,3-hydrogen migration from species **3** (and perhaps also from **2b**). This conjecture was verified in a separate experiment (ESI,† S6.4) involving pure **3** isolated in solid Ar: isomer **5** emerged as an Hg-lamp photolysis product, its presence unambiguously confirmed by comparison to the spectrum of an authentic, matrix-isolated sample of **5** (Fig. 5).

Species **5** may adopt conformations differing by the rotation angle of the PH_2 unit around the C–P bond (Scheme 3). *Gauche* conformers (a pair of enantiomeric species) are 0.34 kcal mol^{-1} lower in energy than *anti* (ESI,† S6.1). Considering the band broadening and matrix-site effects induced by the solid environment, small spectral differences between *gauche* and *anti* species predicted by the DFT calculations (ESI,† S6.2) as well as their limited accuracy, we are unable to distinguish the rotamers in the present spectra. Our separate experiment with Hg-lamp irradiation of matrix-isolated **5** shows the compound to be a photochemical precursor for propargylphosphine, **6**. Species **6** formed out of **5** along with other photodehydrogenation products: HCP, HCCP, HC_3P, and acetylene (ESI,† S6.5).

Propargylphosphine $HC{\equiv}C{-}CH_2{-}PH_2$ (6)

As species **6** lacks any conjugation of π-electrons, with its acetylenic and phosphine moieties separated by a methylene

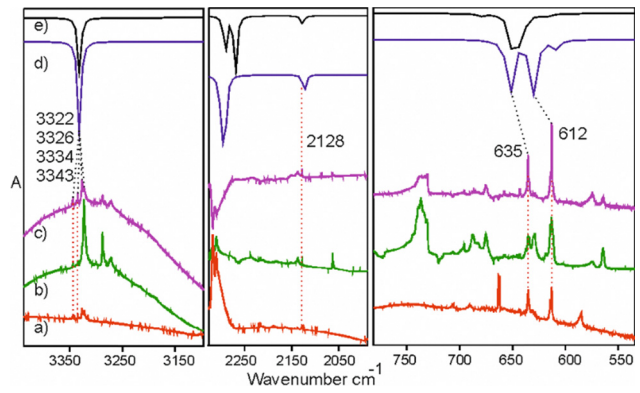

Fig. 6 Identification of **6** among the photolysis products in solid Ar. Trace (a) is the spectrum of an authentic sample of **5** in Ar with **6** as an inseparable admixture. Trace (b) is the difference spectrum (after-minus-before photolysis) showing the net effect of 76 h of Hg-lamp irradiation of **1**. Trace (c) is the difference spectrum showing the net effect of 24 h of Hg-lamp irradiation of **5**. Traces (d) and (e) are B3LYP/aug-cc-pVTZ predictions (frequency scaled by 0.96) for the *anti* and gauche rotamers of **6**, respectively. Wavenumbers of the bands assigned to **6** are provided.

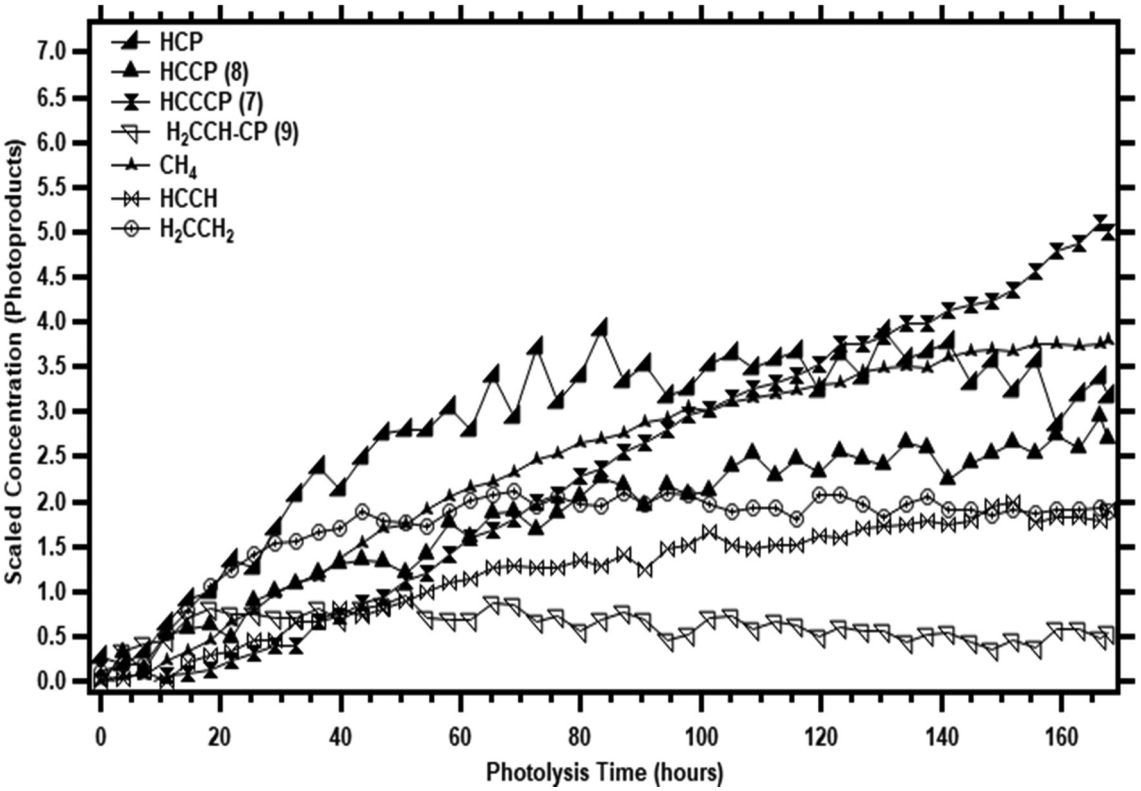

Fig. 7 Evolution of concentrations over the course of 254 nm photolysis of phosphabutyne **1** in solid argon, scaled with respect to the initial concentration of the precursor, taken as 100. Integrated intensities measured for the bands centered at 1524.3 cm^{-1} (7), 564 cm^{-1} (8), 924 cm^{-1} (9), 3271.7 (C_2H_2), 1304.2 (CH_4), 675.5 (HCP) and 950.2 (C_2H_4) were used in conjunction with the B3LYP/aug-cc-pVTZ-derived absolute IR band strengths of 35.7 km mol^{-1} (7), 73.0 km mol^{-1} (8), 44.8 km mol^{-1} (9), 97 km mol^{-1} (C_2H_4), 35 km mol^{-1} (CH_4), 15.7 km mol^{-1} (HCP) and 90 km mol^{-1} (C_2H_2).

unit, one can expect it to be relatively stable towards mid-UV irradiation.

Over the course of photolysis of **1**, the C–H stretching and C–H bending bands of **6** overlap with those of **7** (HC_3P) but the analysis of spectra corresponding to different irradiation times allowed us to separate the spectral features of the two species The authentic spectrum of matrix-isolated **6** was on hand, as the compound was always present as contaminant in the sample of **5**, probably formed as coproduct during the synthesis (Fig. 6). In an Ar matrix, we observe most of the intense IR transitions which match well with the previously reported gas phase spectrum.[35,36]

Analysis of spectra corresponding to different irradiation times allowed us to separate the spectral features of the two species.

Species **6** possesses two stable conformers, *gauche* and *anti* (Scheme 4 and ESI,† S7). According to our DFT prediction, the *gauche* species is just 0.31 kcal mol^{-1} lower in energy than *anti*.

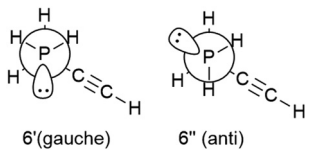

Scheme 4 Rotamers of **6**.

Calculations indicate the expected frequency difference between the two perpendicular acetylenic CH bending modes: 23 cm^{-1} for the *anti* and 8 cm^{-1} for the *gauche* rotamer (ESI,† S7.2). Experimentally, the respective IR bands are separated by 23 cm^{-1}, indicating the dominance of the *anti*-form. Microwave spectroscopy[37] also points to the latter as the preferred form.

Photodissociation

Based on previous experiments[30] with matrix-isolated phosphapropyne, photodehydrogenation is expected to occur along with isomerisation upon irradiation of phosphabutyne. However, bands characteristic of acetylene (3271.2 cm^{-1}), ethylene (950.2 cm^{-1} and 955.3cm^{-1}), and HCP (675 cm^{-1}, 682.2 cm^{-1} and 687 cm^{-1}) indicate the presence of a C–C bond cleaving

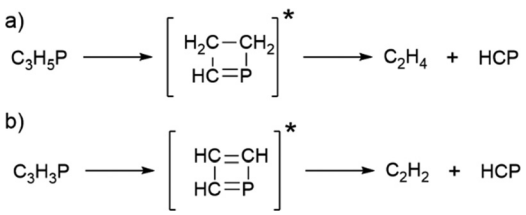

Scheme 5 Proposed mechanism for the formation of HCP, C_2H_4, and C_2H_2 from the isomers of **1** (a) and the C_3H_3P isomer (b).

channel. These species likely form either through retro [2+2] cycloaddition[38] from the isomers (Scheme 5 (a)) and the dehydrogenated products of **1** (Scheme 5 (b)) or through a concerted C–C dissociation during H-migration as C_2H_2/HCP and C_2H_4/HCP complexes in matrix cages. The related C_2H_2/HCN and C_2H_4/HCN adducts,[39,40] in which HCN acts as a H-bond donor to the π-cloud of an unsaturated hydrocarbon, have been observed in low-temperature matrices.

For the complexes formed by HCP with acetylene and ethylene, our calculations reveal weak hydrogen bonding (binding energies below 2.0 kcal mol^{-1}) depicted in Fig. 8: either HCP or a hydrocarbon molecule act as a H-bond donor. The vibrational modes most strongly affected by complexation will be those involved in this interaction. Examining shifts in the C–H stretching and bending of acetylene and HCP as well as the CH_2 waging mode of ethylene compared with the uncomplexed species should indicate the nature of the complex produced in these experiments. A strong blue shift (about 25–40 cm^{-1}) is predicted for the C–H bending frequency of HCP in complexes featuring HCP as the hydrogen bond donor (b and c in Fig. 8 and ESI,† S9). However, compared to the CH bending frequency of uncomplexed HCP (674.03 cm^{-1} gas phase,[5,41] and 672.9 cm^{-1} in solid argon[42]), we observe three bands (675.1 cm^{-1}, 682.2 cm^{-1} and 687.2 cm^{-1}) with shifts of less than 15 cm^{-1}. These shifts suggest the presence of some weaker complexes rather than b and c. Complex formation, whether into a, b, or c, splits the bending mode into out-of-plane and in-plane components, similar to what has recently been reported for the CH bending vibration of an HCP/HCl complex.[42] The shift of out-of-plane CH bending of the C_2H_2/HCl complex is much less (2.8 cm^{-1}) than the shift of in-plane CH bending (21.4 cm^{-1}).[42] In our measurements, we assume that the in-plane bending bands of complexed HCP are those found at 687.2 cm^{-1} (14.3 cm^{-1} shift from uncomplexed molecule) and 682.2 cm^{-1} (9.3 cm^{-1} shift) for C_2H_2/HCP and C_2H_4/HCP, respectively (inset, Fig. 9). The assumption is based on the behaviour of these two peaks over the course of photolysis of **1**: the band at 682.2 cm^{-1} grows at earlier times than the one at 687.2 cm^{-1} (inset, Fig. 9), and Scheme 2 indicates that C_2H_4 is expected before the appearance of C_2H_2. The band at 675.1 cm^{-1} (shifted by +2.2 cm^{-1} with respect to uncomplexed HCP) is presumably due to the out-of-plane bending mode of C_2H_2/HCP. The above picture is consistent with the presence of C_2H_2/HCP complex a, where the discussed HCP bending frequency shift amounts to 7.9 cm^{-1} (B3LYP) or 12.5 cm^{-1} (MP2) for the in-plane mode and only 1.3 cm^{-1} (B3LYP) or 2.0 cm^{-1} (MP2) for the out-of-plane mode.

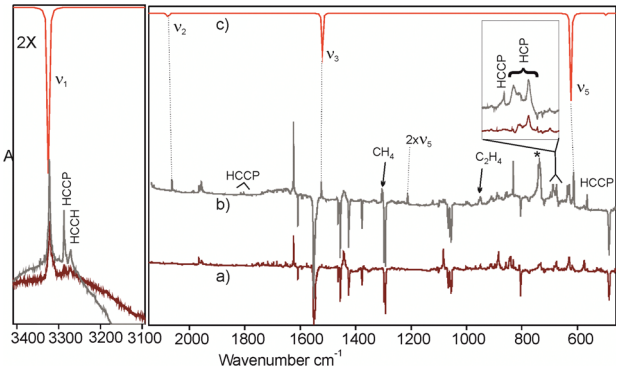

Fig. 9 Identification of the dissociation products observed upon UV photolysis of phosphabutyne (**1**) in solid argon. Traces (a) and (b) are different spectra (after-minus-before photolysis) illustrating the net effect of 3h and 76 h of Hg-lamp irradiation. Topmost trace shows the B3LYP/aug-cc-pVTZ prediction (frequency scaled by 0.96) for the IR spectrum of HC_3P (**7**).

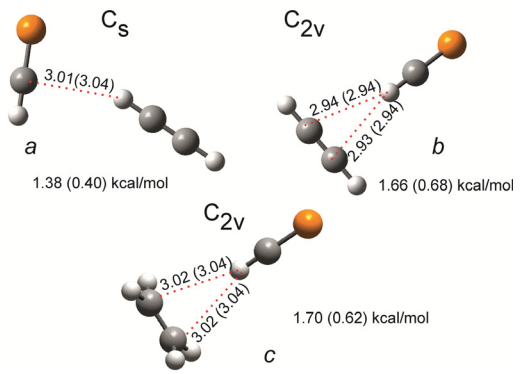

Fig. 8 Complexes of HCP with acetylene and ethylene, as optimized at the MP2/aug-cc-pVTZ and B3LYP/aug-cc-pVTZ (in brackets) level of theory. The BSSE corrected interaction energies and bond length of the weak hydrogen bonds (in Angstrom) are indicated. The point groups symbols of each complex are given.

The complexation-induced shift observed for the CH stretching band of C_2H_2 also points to the presence of complex a in which HCP acts as an H-bond acceptor. The band shifts by −17.7 cm^{-1} from the frequency of 3288.9 cm^{-1} reported for the uncomplexed molecule[43] isolated in solid Ar, while the corresponding shift predicted for a is −14.4 cm^{-1} (B3LYP) or −15.1 cm^{-1} (MP2). For complex b (where HCP acts as an hydrogen bond donor), this shift would, as calculated, be almost doubled. Unfortunately, the CH bending band of C_2H_2 is obscured by a strong feature at 736.6 cm^{-1} caused by the substrate window.

For the C_2H_4/HCP complex, the CH_2 wagging mode of ethylene is observed with shift of +2.1 cm^{-1} and +7.3 cm^{-1} (the splitting is most likely due to matrix sites) with respect to the frequencies of 948 cm^{-1} reported[44] for pure ethylene in solid Ar. The agreement of this shift with B3LYP and MP2 predictions for c (both methods indicate a value around +5 cm^{-1}) is not conclusive, considering the shift in the HCP bending region. Nevertheless, the small observed blue shift in the CH_2 wagging mode of ethylene suggests that HCP is bound to the π-cloud of the ethylene molecule in another orientation than in *c*. To understand the true nature of the C_2H_4/HCP complex, theoretical studies of complexes in argon cages and separate experiments involving solid argon doped with the mixtures of the pure substances are necessary.

The presence of HCCP (**8**) was confirmed based on the reported IR frequencies in an argon matrix.[30] Its formation necessitates the elimination of CH_4, likely from the *P*-methyl alkyne **4** (photoproduced methane is indeed observed here,

Table 1 IR vibrational spectroscopy of HC_3P (**7**)

Mode	Vibrational frequency in cm^{-1} (absolute IR intensity in km mol^{-1})			
	Theory[a] (CCSD(T))/(cc-pVQZ) harmonic	Theory[b] (B3LYP/aug-cc-pVTZ) harmonic	Theory[c] (VPT2//B3LYP/aug-cc-pVTZ) anharmonic	Ar matrix
C–H str. (ν_1)	3453	3324.7(102)	3337.7(113.6)	3322.7
C–C str. (ν_2)	2111	2076.0(8.7)	2119.5(12.1)	2062.8
C–P str. (ν_3)	1544	1519.8(35.8)	1563.1(91.2)	1524.3
HCCCP str. (ν_4)	687	680.4(0.2)	708.7(0.8)	—
C–H bend. (ν_5)	621	622.2(80.4)	635.0(513.8)	611.2 611.8 614, 613.1
CCP bend. (ν_6)	479	496.5(0.7)	514.0(5.4)	—
CCP bend. (ν_7)	192	196.6(7.9)	205.4(152.1)	—
Overtone ($2\nu_5$)	—	—	1276.6 (93.8) 1255.5 (46.9)	1212.2

[a] Harmonic approximation, not scaled (ref. 45). [b] Scaling factor 0.96 (this work). [c] This work.

through its band at 1304.6 cm^{-1}). Growth curves for the two species (Fig. 7) are consistent with the assumption of their common origin, considering inevitable inaccuracies in the computed absolute IR intensities. No bands attributable to any other phosphinidene (a compound bearing a formally single C–P bond) were detected.

Three stretching fundamental vibrational frequencies, one bending fundamental, and one bending overtone of HC_3P (**7**) are identified (Table 1 and Fig. 9 and 10). Anharmonic calculations confirm the high strength of the detected C–H bending overtone band (ESI,† S11). While the exact dehydrogenation pathways leading from **1** to **7** remain to be elucidated, the high and constantly growing concentration of HC_3P suggests that the immediate precursor for **7** swiftly reaches a steady state and that **7** does not undergo any significant secondary photolysis.

A series of additional experiments were conducted photolyzing Ar-matrix isolated compounds **1**, **3**, and **5** with far-UV (160–190 nm) radiation from a microwave-driven Xe lamp (Fig. 10). All of these far-UV photolyses produced **7** as the major

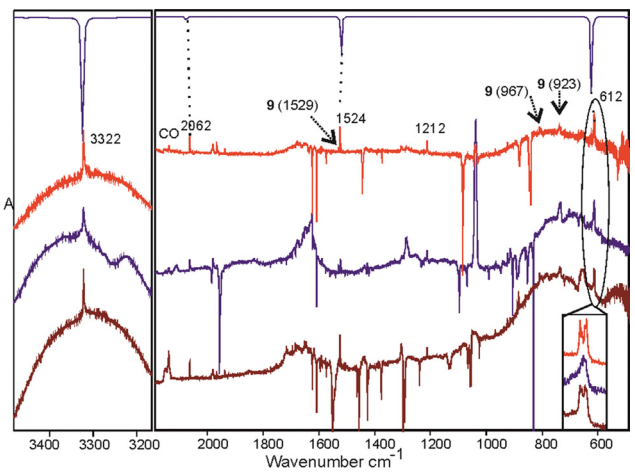

Fig. 10 Difference spectra depicting the identification of HC_3P (**7**) among the products generated by far-UV photolyses (160–190 nm, 6-hour irradiations) of Ar-matrix isolated compounds **1** (bottommost, brown trace), **3** (red), and **5** (blue). Top: B3LYP/aug-cc-pVTZ prediction for the IR spectrum of **7** (frequency scaled by 0.96).

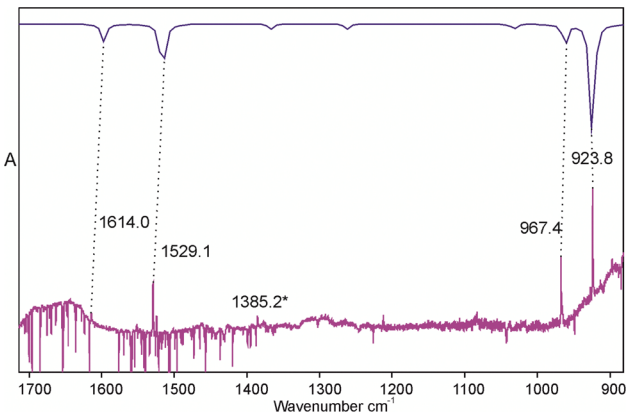

Fig. 11 Bottom: Difference spectrum (after-minus-before photolysis) showing, for phosphabutyne **1** in solid Ar, the net effect of an additional 24 h irradiation at 308 nm after 6 days of 254 nm photolysis. Top: B3LYP/aug-cc-pVTZ prediction for the IR spectrum of **9** (frequency scaled by 0.96). Asterisked assignment is tentative.

product. The only C_3H_3P species detected here is vinylphosphaethyne (CH_2CHCP, **9**). It was difficult to identify following Hg-lamp and far-UV irradiation due to the weakness of its bands. Unambiguous assignment was only possible by performing a secondary photolysis using 308 nm light following photolysis at 254 nm (Fig. 11 and ESI,† S8). The identified IR frequencies are: 923.8 cm^{-1} (CH_2 wagging), 967.4 (CH_2 and CH twisting), 1529.1 cm^{-1} (C–P stretching), and 1614.0 cm^{-1} (C–C stretching). Molecule **9** is one probable precursor for **7**.

Conclusions

Photolysis of Ar matrix-isolated phosphabutyne, CH_3–CH_2–C≡P, with 254 nm radiation produces a variety of C_3H_5P isomers as well as photodissociation products. Isomers observed include CH_2=C=P–CH_3, CH_3–CH=C=PH, HC≡C-PH–CH_3 (tentative), HC≡C–CH_2–PH_2, CH_3–C≡C–PH_2, and CH_2=C=CH–PH_2. Formation of HCP, ethylene, and acetylene indicates that some of the isomers undergo a retro-cycloaddition reaction. Photodissociation consists mainly of

the elimination of methane (leading to HCCP) and in dehydrogenation resulting in the formation of phosphabutadiyne (H–C≡C–C≡P) and vinylphosphaethyne (CH_2═CH–C≡P). These experiments gave access, for the first time, to the infrared spectra of HC_3P, CH_2CHCP, and CH_3–CH═C═P. Five vibrational frequencies, including a bending overtone, of phosphabutadiyne (HC_3P), the phosphorus analog of the astrochemically significant cyanoacetylene, were determined. A simplified reaction scheme was proposed, the verification of which, as well as a full description of the photochemical transformations of phosphabutyne, require dedicated quantum chemical studies.

Materials and methods

Diethylene glycol dibutyl ether (diglyme), tetraethylene glycol dimethyl ether (tetraglyme), lithium aluminum hydride, aluminum chloride, 1,8-diazabicyclo[5.4.0]undec-7-ene (DBU), *n*-butyl lithium (*n*-BuLi) (2.5 M in hexanes) and ethyl bromide ($CH3CH_2Br$) were purchased from the Aldrich Company and used without further purification.

Synthesis

Phosphabutyne **1** was prepared in a three-step reaction following reported procedures (Scheme 6).[46,47] Briefly, (1,1,1-trichloromethyl) phosphonic acid, diisopropyl ester was reacted with *n*-BuLi in the presence of LiCl before the addition of ethyl bromide to give (1,1-dichloropropyl)phosphonic acid, diisopropyl ester.[47] In a chemoselective reduction with $AlHCl_2$ in a high boiling solvent, diglyme, the 1,1-dichloropropylphosphine was formed, isolated at low pressure with gentle heating of the reaction mixture and condensed in a cold trap.[48] The synthesis of phosphabutyne by bis-dehydrochlorination of the phosphine was performed at low temperature in diglyme, using the strong Lewis base 1,8-diazabicyclo[5.4.0]undec-7-ene (DBU). For the two last steps, the product was isolated from the crude reaction mixture in a vacuum line by selective trapping at 183 K and 77 K, respectively.

1-Propynylphosphine **3** and 1,2-propadienylphosphine **5** were synthesized as previously reported.[48]

Matrix isolation experiments

Precursor compounds were sublimed into an evacuated stainless-steel manifold and diluted with argon at approx. 1 : 1000 ratio using standard manometric techniques. The gas mixture was condensed on a cold (*ca.* 10 K) cesium iodide window mounted to a closed-cycle helium cryostat (Advanced Research Systems DE-202SE refrigerator, ultimate temp. of 6 K) and exposed to radiation of a low-pressure Hg-lamp, dominated by resonance emission at 254 nm. A microwave-driven xenon lamp (Opthos instrument Co.) was used as a VUV continuum radiation source (150–190) nm. Photolysis progress was monitored using a Bruker Vertex 70 Fourier transform spectrometer featuring liquid nitrogen cooled MCT detector operating at its maximal resolution of 0.16 cm^{-1}.

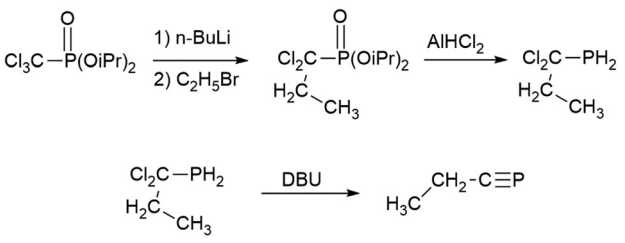

Scheme 6 Synthesis of phosphabutyne **1**.

Computational methods

Equilibrium molecular structures and the corresponding harmonic vibrational frequencies of molecular vibrations (as given by analytical second derivatives of the total energy, with respect to nuclear positions) were predicted at the DFT level employing the B3LYP functional[49] and aug-cc-pVTZ basis set.[50,51] The derived vibrational frequencies were scaled by a factor of 0.96 to take partial account of anharmonicity, incomplete inclusion of electron correlation effects, and deficiencies in the applied basis set. Zero-point energy correction was applied to the obtained electronic energy values. Default convergence criteria were used. For non-covalent complexes, the equilibrium geometry and IR frequencies were obtained from both Møller–Plesset perturbation theory of second order (MP2)[52] and density functional theory (DFT) method with the B3LYP hybrid functional. The binding energies of the complexes were corrected for the basis set superposition errors (BSSE) using the counterpoise (CP) scheme of Boys and Bernardi.[53] All computations were performed using the Gaussian 16 software suite.[54]

Data availability

The authors confirm that the data supporting the results of this research article are available in the article and its ESI.†

Conflicts of interest

There are no conflicts to declare.

Acknowledgements

We acknowledge the financial support from the PHC Polonium project no. BPN/BFR/2021/1/00028/U/00001. J. C. G. thanks for the support from ''Programme National Physique et Chimie du Milieu Interstellaire'' (PCMI) of CNRS/INSU with INC/INP co-funded by CEA and CNES.

Notes and references

1 M. Regitz, *Chem. Rev.*, 1990, **90**, 191–213.
2 J. F. Nixon, *Chem. Soc. Rev.*, 1995, **24**, 319–328.
3 M. Regitz, *J. Heterocycl. Chem.*, 1994, **31**, 663–677.
4 K. Nakajima, S. Takata, K. Sakata and Y. Nishibayashi, *Angew. Chem., Int. Ed.*, 2015, **54**, 7597–7601.
5 T. E. Gier, *J. Am. Chem. Soc.*, 1961, **83**, 1769–1770.

6 J. C. T. R. Burckett St. Laurent, T. A. Cooper, H. W. Kroto, J. F. Nixon, O. Ohashi and K. Ohno, *J. Mol. Struct.*, 1982, **78**, 215–220.
7 H. W. Kroto, J. F. Nixon and K. Ohno, *J. Mol. Spectrosc.*, 1981, **90**, 512–516.
8 K. Ohno, H. W. Kroto and J. F. Nixon, *J. Mol. Spectrosc.*, 1981, **90**, 507–511.
9 L. Bizzocchi, S. Thorwirth, F. Lewen and G. Winnewisser, *J. Mol. Spectrosc.*, 2001, **205**, 110–116.
10 U. Bergstraesser, *Sci. Synth.*, 2004, **18**, 427–444.
11 E. A. Cohen, G. A. McRae, H. Goldwhite, S. Di Stefano and R. A. Beaudet, *Inorg. Chem.*, 1987, **26**, 4000.
12 J. P. Albrand, S. P. Anderson, H. Goldwhite and L. Huff, *Inorg. Chem.*, 1975, **14**, 570–572.
13 W. J. Marshall, B. M. Fish, M. F. Schiffhauer, F. Davidson and C. N. McEwen, *Organometallics*, 2009, **28**, 2410–2416.
14 G. Becker, G. Gresser and W. Whl, *Z. Naturforsch., B*, 1981, **36**, 16.
15 M. Regitz, *Chem. Rev.*, 1990, **90**, 191–213.
16 C. M. Walmsley, G. Winnewisser and F. Toelle, *Astron. Astrophys.*, 1980, **81**, 245–250.
17 H. E. Matthews and T. J. Sears, *Astrophys. J.*, 1983, **272**, 149–153.
18 M. Guélin, J. Cernicharo, G. Paubert and B. E. Turner, *Astron. Astrophys.*, 1990, **230**, L9–11.
19 M. Agúndez, J. Cernicharo and M. Guélin, *Astron. Astrophys.*, 2014, **570**, A45.
20 M. Agúndez, J. Cernicharo and M. Guélin, *Astrophys. J.*, 2007, **662**, L91–L94.
21 R. Appel, F. Knoch and V. Winkhaus, *Chem. Ber.*, 1986, **119**, 2466–2472.
22 G. Märkl, P. Kreitmeier, H. Nöth and K. Polbom, *Angew. Chem., Int. Ed. Engl.*, 1990, **29**, 927–929.
23 M. Yoshifuji, K. Toyota, K. Shibayama and N. Inamoto, *Tetrahedron Lett.*, 1984, **25**, 1809–1812.
24 G. Märkl and S. Reitinger, *Tetrahedron Lett.*, 1988, **29**, 463–466.
25 G. Märkl and U. Herold, *Tetrahedron Lett.*, 1988, **29**, 2935–2938.
26 H. W. Kroto, J. F. Nixon and K. Ohno, *J. Mol. Spectrosc.*, 1981, **90**, 367–373.
27 L. Margules, J. Demaison, P. B. Sreeja and J.-C. Guillemin, *J. Mol. Struct.*, 2006, **238**, 234–240.
28 B. Pellerin, P. Guenot and J.-M. Denis, *Tetrahedron Lett.*, 1987, **28**, 5811–5814.
29 J.-C. Guillemin, T. Janati and J.-M. Denis, *J. Chem. Soc., Chem. Commun.*, 1992, 415–416.
30 A.-L. Lawzer, T. Custer, J.-C. Guillemin and R. Kołos, *Angew. Chem., Int. Ed.*, 2021, **60**, 6400–6402.
31 R. A. Moss, *Chem. Rev.*, 2013, **113**(9), 6903–6904.
32 B. Lu and X. Zeng, *Chem. – Eur. J.*, 2024, e202303283.
33 J.-P. Maillard, *Philos. Trans. R. Soc., A*, 2024, **382**, 20230070.
34 J.-C. Guillemin, T. Janati, J.-M. Denis, P. Guenot and P. Savignac, *Tetrahedron Lett.*, 1994, **35**, 245–248.
35 R. H. Shay, B. N. Diel, D. M. Schubert and A. D. Norman, *Inorg. Chem.*, 1988, **27**, 2378–2382.
36 J.-C. Guillemin and K. Malagu, *Organometallics*, 1999, **18**, 5259–5263.
37 J. Demaison, J.-C. Guillemin and H. Mollendal, *Inorg. Chem.*, 2001, **40**, 3719–3724.
38 F. Mathey and P. Le Floch, *J. Org. Chem.*, 2004, **69**, 5100–5103.
39 A. Toumi, I. Couturier-Tamburelli, T. Chiavassa and N. Pietri, *J. Phys. Chem. A*, 2014, **118**, 2453–2462.
40 A. Toumi, N. Pietri and I. Couturier-Tamburelli, *Phys. Chem. Chem. Phys.*, 2015, **17**, 30352–30363.
41 M. Jung, B. P. Winnewisser and M. Winnewisser, *J. Mol. Spectrosc.*, 1997, **413**, 31–48.
42 J. Jiang, B. Lu, B. Zhu, G. Rauhut and X. Zeng, *J. Phys. Chem. Lett.*, 2023, **14**, 4327–4333.
43 K. Sundararajan and N. Ramanathan, *J. Mol. Spectrosc.*, 2009, **920**, 369–376.
44 E. Rytter and D. M. Gruen, *Spectrochim. Acta, Part A*, 1979, **35A**, 199–207.
45 L. Bizzocchi, C. D. Esposti and P. Botschwina, *Chem. Phys. Lett.*, 2000, 411–417.
46 J.-C. Guillemin, T. Janati and J.-M. Denis, *J. Org. Chem.*, 2001, **66**, 7864–7868.
47 C. Grandin, E. About-Jaudet, N. Collignon, J.-M. Denis and P. Savignac, *Heteroat. Chem.*, 1992, **3**, 337–343.
48 J.-C. Guillemin, P. Savignac and J.-M. Denis, *Inorg. Chem.*, 1991, **30**, 2170–2173.
49 A. D. Becke, *J. Chem. Phys.*, 1993, **7**, 5648–5652.
50 D. E. Woon and T. H. Dunning Jr., *J. Chem. Phys.*, 1993, **98**, 1358–1371.
51 K. A. Peterson, *J. Chem. Phys.*, 2003, **119**, 11099–11112.
52 C. Møller and M. S. Plesset, *Phys. Rev.*, 1934, **46**, 618–622.
53 S. F. Boys and F. Bernardi, *Mol. Phys.*, 1970, **19**, 553–566.
54 M. J. Frisch, G. W. Trucks, H. B. Schlegel, G. E. Scuseria, M. A. Robb, J. R. Cheeseman, G. Scalmani, V. Barone, G. A. Petersson, H. Nakatsuji, X. Li, M. Caricato, A. V. Marenich, J. Bloino, B. G. Janesko, R. Gomperts, B. Mennucci, H. P. Hratchian, J. V. Ortiz, A. F. Izmaylov, J. L. Sonnenberg, D. Williams-Young, F. Ding, F. Lipparini, F. Egidi, J. Goings, B. Peng, A. Petrone, T. Henderson, D. Ranasinghe, V. G. Zakrzewski, J. Gao, N. Rega, G. Zheng, W. Liang, M. Hada, M. Ehara, K. Toyota, R. Fukuda, J. Hasegawa, M. Ishida, T. Nakajima, Y. Honda, O. Kitao, H. Nakai, T. Vreven, K. Throssell, J. A. Montgomery, Jr., J. E. Peralta, F. Ogliaro, M. J. Bearpark, J. J. Heyd, E. N. Brothers, K. N. Kudin, V. N. Staroverov, T. A. Keith, R. Kobayashi, J. Normand, K. Raghavachari, A. P. Rendell, J. C. Burant, S. S. Iyengar, J. Tomasi, M. Cossi, J. M. Millam, M. Klene, C. Adamo, R. Cammi, J. W. Ochterski, R. L. Martin, K. Morokuma, O. Farkas, J. B. Foresman and D. J. Fox, *Gaussian 16, Revision B.01*, Gaussian, Inc., Wallingford CT, 2016.